

Quantification des dommages causés par un impact à faible vitesse dans les stratifiés composites à l'aide de l'imagerie par impulsion térahertz

Quantification of Low Velocity Impact Damage in Composite Laminates with Terahertz Pulsed Imaging

P. Pomarède¹, N. Miquoi¹, D.S. Citrin^{2,3}, F. Meraghni¹ and A. Locquet^{2,3}

1 : Arts et Métiers Institute of Technology, CNRS, Université de Lorraine, LEM3-UMR 7239 CNRS
4 rue Augustin Fresnel, 57078 Metz, France
e-mail: pascal.pomarede@ensam.eu, fodil.meraghni@ensam.eu

2 : Georgia Tech-CNRS IRL2958
Georgia Tech-Europe, 2 Rue Marconi, 57070 Metz, France
e-mail: alocquet@georgiatech-metz.fr, david.citrin@ece.gatech.edu

3 : School of Electrical and Computer Engineering,
Georgia Institute of Technology, Atlanta, GA, 30332-0250, USA
e-mail: alocquet@georgiatech-metz.fr, david.citrin@ece.gatech.edu

Résumé

Cette étude utilise l'imagerie par impulsion térahertz pour détecter les dommages causés par des impacts à faible vitesse sur des stratifiés en polyamide renforcé de fibres de verre. L'objectif est d'étudier la fiabilité de l'imagerie térahertz pour la détection des dommages et l'évaluation des matériaux composites, afin de promouvoir son utilisation dans l'industrie. Différentes énergies d'impact sont testées pour observer comment les dommages commencent et se propagent. Les indentations permanentes, qui indiquent des dommages, sont mesurées par imagerie térahertz et confirmées par profilométrie. La gravité des dommages, montrée par le nombre de couches fissurées, est également identifiée par imagerie térahertz et vérifiée par tomographie par rayons X. L'étude révèle un lien fort entre la taille des bosses et l'étendue des dommages, suggérant que l'imagerie térahertz est une méthode fiable pour détecter et évaluer la gravité des dommages dus aux impacts dans ces matériaux.

Abstract

This study uses terahertz pulse imaging to detect damage from low-speed impacts on glass-fiber reinforced polyamide laminates. The objective is to study the reliability of terahertz imaging for damage detection and evaluation of composite materials to promote its use in the industry. Different impact energies are tested to see how damage starts and spreads. Permanent indents, which indicate damage, are measured with terahertz imaging and confirmed with profilometry. The severity of the damage, shown by the number of cracked layers, is also identified using terahertz imaging and verified with X-ray tomography. The study finds a strong link between the size of the dents and the extent of the damage, suggesting that terahertz imaging is a reliable way to detect and evaluate the severity of impact damage in these materials.

Mots Clés : Composite renforcé de fibres tissées; Contrôle Non Destructive; Imagerie par impulsion térahertz; Détection de l'endommagement; Impact à faible énergie

Keywords: Woven fiber reinforced composite; Non-Destructive Evaluation; Terahertz pulse imaging; Damage detection; Low-velocity impact

1. Introduction

Under thermomechanical stress, these composites can suffer from various types of damage, such as matrix cracking, interface debonding, fiber breakage, and delamination, especially as thickness increases [1–4]. One challenging type of damage to assess is from low-velocity impacts, which may not be visible on the surface but can cause internal damage known as barely visible impact damage (BVID) [3]. This type of damage is a key concern in nondestructive evaluation (NDE) because it can lead to progressive degradation and significantly reduce the lifespan and performance of the composite material [5–7].

For low-velocity but high-momentum impacts, the impactor can leave a permanent indentation (PI) on the structure. However, this mark is usually hard to spot during regular visual inspections. The depth and size of the PI depend on the impact energy and the resulting internal damage [8,9]. It can also signal the start of damage, even within the barely visible impact damage (BVID) range [10]. Therefore, PI is a useful indicator for assessing the severity of damage.

There is a crucial need to develop new nondestructive evaluation (NDE) methods to detect and measure damage in composites. The goals are to (i) measure permanent indentation (PI) marks on impacted surfaces, even in the barely visible impact damage (BVID) range, and (ii) detect and quantify internal damage mechanisms. Several NDE techniques have been explored, including X-ray tomography [11,12], thermography [13], and ultrasound [9,14,15]. Each method has its advantages and disadvantages, and the choice depends on factors like cost, damage size, safety, efficiency, and portability [16–18]. X-ray tomography offers high resolution but is time-consuming and poses health risks due to ionizing radiation. Thermography is faster but has lower resolution. Ultrasound provides a balance between inspection time and resolution, though its effectiveness can vary depending on the specific method used.

Terahertz (THz) imaging has become a promising method for detecting and evaluating damage in composites. THz waves, which range from 100 GHz to 10 THz, lie between microwaves and infrared light. This technique is noninvasive, noncontact, and nonionizing, making it safe for inspecting electrically insulating materials. It offers better depth resolution than ultrasound [19] and avoids the health risks associated with X-ray tomography [20]. Additionally, commercial THz imaging systems are now compact, robust, and increasingly affordable, making them suitable for in-service inspections. THz imaging has been used to measure fiber orientation [21,22], characterize composite materials [23], and detect various types of damage, including delamination [24], fatigue [25], and heat damage [26]. Previous studies [19,27,28] have looked at low-velocity impact damage, but they often focused only on surface damage or a single impact energy. To develop a practical tool for industrial use, it's important to study a wider range of impact energies and thoroughly examine internal damage to confirm that permanent indentation (PI) is a reliable indicator of damage severity.

In this study, we examine woven glass-fiber composite laminates impacted at seven different low-impact energies. These energies fall within the Barely Visible Impact Damage (BVID) range. We use terahertz (THz) imaging to analyze the samples. First, we measure the permanent indentation (PI) on the surface using THz imaging and compare these results with other methods. Next, we perform THz imaging on the impacted samples to get both surface and depth information, assessing the severity of the damage. We also use X-ray tomography to validate the THz findings and understand how the damage area changes with impact energy. Finally, we establish a link between the progression of PI and the internal damage detected in the samples. Our results demonstrate that THz imaging is effective for damage detection and evaluation in composite material components both in the workshop and during service.

2. Materials and methods

The material studied is a semi-crystalline co-polyamide 66/6, reinforced with three layers of 2/2 twill woven glass fibers, totaling 1.53 mm in thickness. The fibers are oriented at 0°/90° for balanced reinforcement and are manufactured by DuPont. Detailed structural characterization of this material is available in recent studies [9,14]. The composite, with a thickness of 1.53 mm, has a fibre weight ratio of 63 % corresponding to a fiber volume fraction of 43 %.

Impact tests are conducted using a drop-weight machine with a 16-mm diameter hemispherical impactor weighing 1.02 kg. The setup includes a piezoelectric load sensor, two laser displacement sensors, and a data acquisition system. Eight samples (100 x 150 x 1.53 mm³) are tested, with plates clamped at both ends. The impactor height varies to produce seven energy levels: 8.5, 13.1, 13.7, 14.2, 15.7, 18.1, 23, and 25 J. An undamaged sample is used as a control

A THz time-domain spectroscopy (THz-TDS) system (TeraView Ltd. TPS Spectra 3000) is used for all THz measurements in this study. The setup, generates THz pulses from 60 GHz to 3 THz, with signals averaged over 5 shots per time delay per pixel. An xy scanner images a 60 x 60 mm² region with 0.2 mm spatial steps. After recording the data, noise is reduced using a 0.2 THz high-pass filter and wavelet denoising. The wavelet transform applies low and high-pass filters along the time axis for each chosen decomposition level, yielding approximate and detail coefficients. Coefficients with small values, considered noise, are removed through soft thresholding and signal reconstruction. In this work, symlet 4 wavelets with a maximum level of 7 are used. The B and C-scans are averaged within a five-pixel radius.

3. Measurement of the Permanent Indentation depth using optical profilometry and terahertz imaging

After an impact test, the impactor leaves a permanent indentation (PI) on the surface. The PI depth increases with impact energy and shows the level of internal damage. In this section, PI depth is measured using two techniques: optical profilometry for reference and THz imaging in reflection. For both methods, the PI location is identified first, then the maximum depth is measured.

Optical profilometry measurements are taken using a LEICA DCM3D with 5x magnification and a scan size of 27 x 20.23 mm². This setup provides a lateral resolution of 0.94 μm and a vertical resolution of less than 150 nm. All seven impacted samples are scanned, and the surface texture maps are post-processed with Leica Maps software. Figure 1 shows how PI depth changes with impact energy. Three stages are identified: initially, PI depth increases slightly to about 25 μm at 14.2 J. Then, it stabilizes until 18.1 J. Finally, PI depth increases significantly, reaching 144 μm.

Then the PI depth is extracted from terahertz imaging. To do so, the time of arrival of the first positive peak is extracted from the time signal. Using the C-scan help narrowing the investigated area. All the PI measured are shown in Figure 1. Good agreement with the results from optical profilometry is observed, establishing the suitability of the THz imaging as a resolved measurement of the PI.

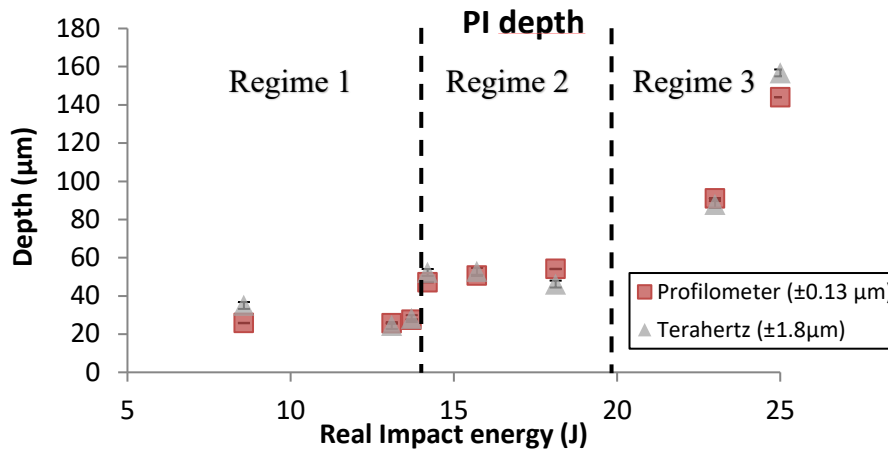


Figure 1: Comparison of PI depth using optical profilometry and THz imaging shows that both methods largely agree and reveal three impact-energy regimes. Initially, PI depth increases with impact energy, then stabilizes, and at high impact energy, PI depth increases significantly.

4. Investigation of the internal damage using terahertz imaging

Besides PI, impact loading can cause other types of damage in a composite laminate. Thin plates tend to bend during impact, with damage starting on the opposite side and spreading inside the sample. This section investigates these damage mechanisms and compares them with the PI depth discussed earlier. Impacted samples are first examined with X-ray tomography for high-resolution comparison and as a reference for THz results. As observed in Figure 2, the intersection of the 0° and 90° yarns creates a local refractive-index mismatch between the matrix and fabric reinforcement, increasing the amplitude. This means that even without PI or internal damage, the composite microstructure can produce complex THz B-scans that are difficult to interpret. Therefore, analyzing internal damage in this material requires a detailed comparison with an undamaged sample.

Except for creating a PI on the impacted surface, the lowest impact energies do not cause noticeable damage in the samples; nothing is visible in THz or X-ray tomography results. At higher impact energy, the first damage mechanism observed is matrix cracking on the opposite surface after 14.2 J. At 18.1 J, additional damage mechanisms begin to occur, leading to the initiation of delamination.

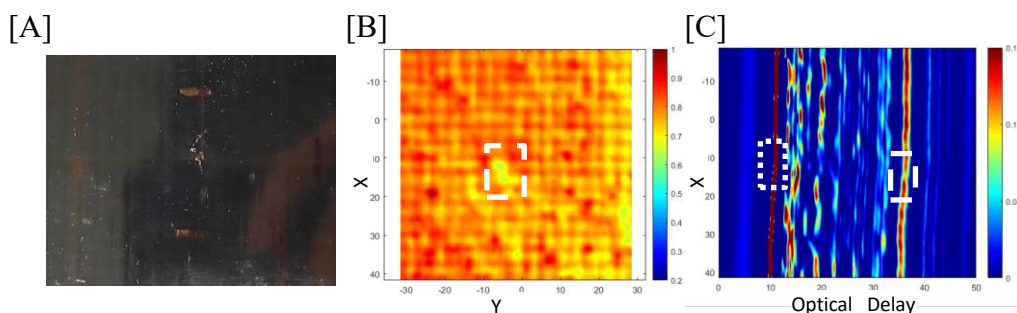


Figure 2: Analysis of the sample impacted at 14.2 J. [A]: Photograph of the non-impacted surface showing matrix cracking (dashed box). [B]: THz C-scan of the non-impacted surface showing matrix cracking as decreased amplitude. [C]: THz B-scans showing damage mechanisms: dotted box for PI, dashed box for bottom surface cracking.

At 23 J, a crack network forms on the non-impacted side and spreads to the second layer. This is shown in X-ray tomography and highlighted in white in Figure 3. THz images also detect the

propagation of the damage area (Figure 3). The impact region is clearly visible around 17 ps and $x = 20$ mm. Small delamination near the non-impacted side shows as a local increase in amplitude (white dashed box). Similar amplitude increases in the second layer (solid-line box) are also noted. High impact energy causes visible layer deformation inside the material, not just on the surface, appearing as ripples in the white box in Figure 3.

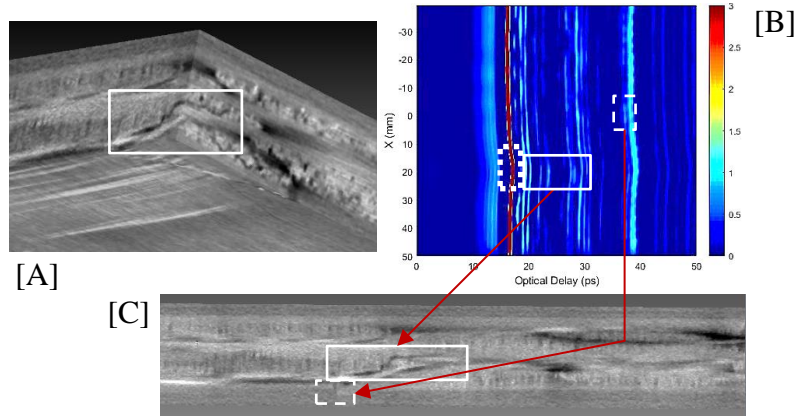


Figure 3: Analysis of the sample impacted at 23 J. [A]: X-ray tomography image showing a crack propagating to the second ply. [B]: THz B-scan near the impacted region. [C]: X-ray tomography image near the impacted region. Multiple types of damage are visible: dotted box for Permanent Indentation (PI), dashed box for bottom surface cracks, and solid line box for delamination in the third layer.

At 25 J impact energy, the damage extends to the third layer, as shown in X-ray tomography in Figure 4. These figures reveal matrix cracking and delamination in various layers, connected to each other, showing matrix cracking starting from the non-impacted surface and spreading towards the impacted surface. THz B-scans reveal delamination between layers as local amplitude increases, highlighted by solid-line boxes in Figure 4. Matrix cracking on the impacted surface also occurs, but the first echo's large amplitude causes saturation in the figures. Similar observations are seen in the THz B-scans of Figure 4. Matrix cracks and delamination propagate from the non-impacted to the impacted surface, and cracks are detected near the sample's outer surfaces.

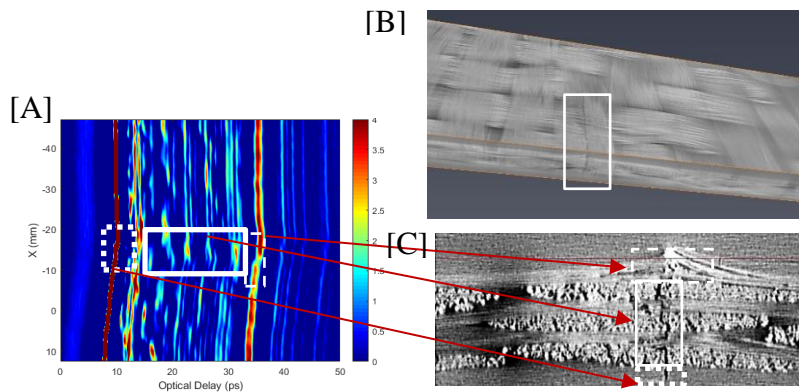


Figure 4: Analysis of the sample impacted at 25 J. A: THz B-scan near the impacted region. B: X-ray tomography image showing matrix cracks running from the non-impacted surface to the other in 3D. C: Longitudinal slice of the X-ray tomography image. Various damage types are visible: dotted box for permanent indentation (PI) + matrix cracks, dashed box for cracks on the bottom surface, and solid line box for delamination.

5. Discussion

THz imaging shows damage initiation and propagation, providing a scenario of progressive material degradation. All chosen impact energies create a PI on the impacted surface. From 8.5 to 13.7 J, no additional damage occurs. At 14.2 J, matrix cracking is visible on the non-impacted surface, with a significant increase in PI depth. The size of the matrix cracks and PI depth increases with impact energy. At 18.1 J, delamination begins between surface plies on the non-impacted side, with PI depth stabilizing until this level. After 18.1 J, PI depth increases drastically, matching the growth of the damage area. Cracks propagate deeper into the sample at 23 J and 25 J. Figure 5 summarizes this damage scenario, corresponding impact-energy levels, and PI depths.

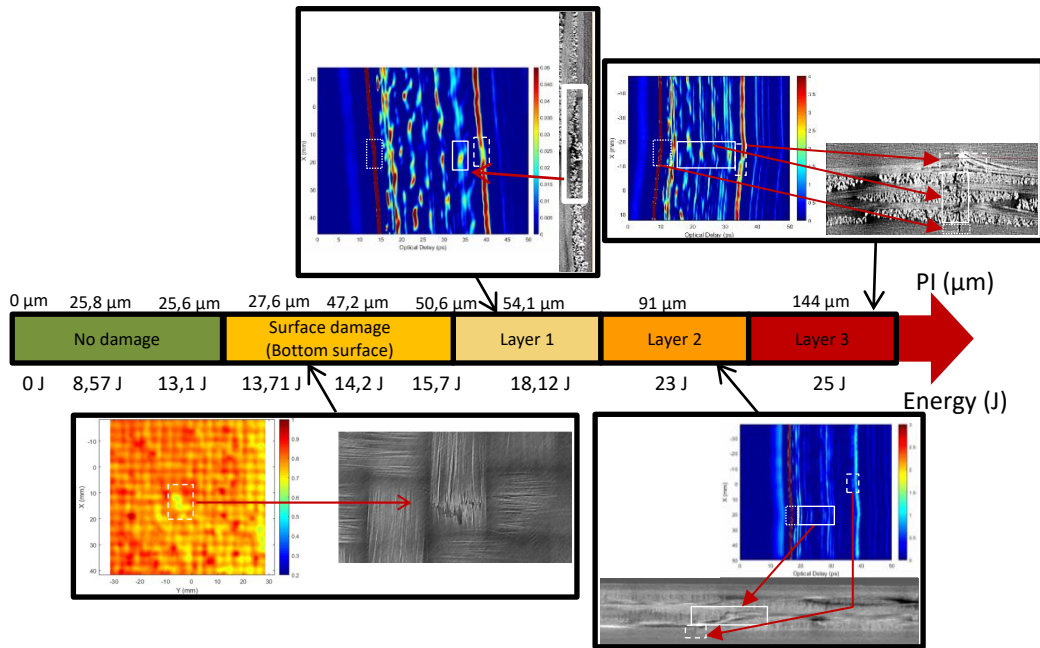


Figure 5: Summary of the damage scenario for the studied material during impact events. The propagation of damage through the sample is indicated. Impact energy and PI depth are also provided.

6. Conclusion

This study examines the capability of THz imaging to detect and quantify permanent indentations (PI) on the surface of an impacted woven-fabric composite laminate and the induced damage. Various impact energy levels, near the BVID range, were used to explore realistic defects. THz images revealed damage mechanisms such as matrix cracking, delamination, and crack networks, which were confirmed by X-ray tomography. PI depth measurements, which increase with impact energy, aligned with optical profilometry results. THz PI depth measurement is thus a potential method for assessing the criticality of induced damage. The composite material's complex reinforcement and microstructure make it challenging to analyze with THz radiation. This complicates image interpretation for human operators, particularly at low damage levels. In the future, machine-learning approaches may help with defect identification in THz imaging. Preliminary works has already been undergone by our teams.

7. ACKNOWLEDGEMENTS

A.L. and D.S.C. acknowledge the financial support of the Région Grand Est. A.L and D.S.C. thank the CPER SusChemProc. A.L, D.S.C., P.P, and F.M acknowledge financial support from Institut Carnot ARTS. D.R acknowledge the support of the Chair in Photonics.

8. References

- [1] M. Karayaka, P. Kurath, Deformation and Failure Behavior of Woven Composite Laminates, *J. Eng. Mater. Technology* 116 (1994) 222–232.
- [2] J. Montesano, Z. Fawaz, H. Bougherara, Non-destructive assessment of the fatigue strength and damage progression of satin woven fiber reinforced polymer matrix composites, *Compos. Part B Eng.* 71 (2015) 122–130. <https://doi.org/10.1016/j.compositesb.2014.11.005>.
- [3] S. Agrawal, K.K. Singh, P.-K. Sarkar, Impact damage on fibre-reinforced polymer matrix composite – A review, *J. Compos. Mater.* 48 (2013) 317–332. <https://doi.org/10.1177/0021998312472217>.
- [4] S. Gul, I.E. Tabrizi, B.S. Okan, A. Kefal, M. Yildiz, An experimental investigation on damage mechanisms of thick hybrid composite structures under flexural loading using multi-instrument measurements, *Aerosp. Sci. Technol.* 117 (2021) 106921. <https://doi.org/10.1016/j.ast.2021.106921>.
- [5] M. Kara, K. Muhammed, Effects of the number of fatigue cycles on the impact behavior of glass fiber / epoxy composite tubes, *Compos. Part B Eng.* 123 (2017) 55–63. <https://doi.org/10.1016/j.compositesb.2017.04.021>.
- [6] C. Atas, O. Sayman, An overall view on impact response of woven fabric composite plates, *Compos. Struct.* 82 (2008) 336–345. <https://doi.org/10.1016/j.compstruct.2007.01.014>.
- [7] P. Marguères, F. Meraghni, Damage induced anisotropy and stiffness reduction evaluation in composite materials using ultrasonic wave transmission, *Compos. Part A Appl. Sci. Manuf.* 45 (2013) 134–144. <http://www.sciencedirect.com/science/article/pii/S1359835X12002977> (accessed December 11, 2014).
- [8] S.Z.H. Shah, S. Karuppanan, P.S.M. Megat-yuso, Z. Sajid, Impact resistance and damage tolerance of fiber reinforced composites : A review, 217 (2019) 100–121. <https://doi.org/10.1016/j.compstruct.2019.03.021>.
- [9] N. Miquoi, P. Pomarède, F. Meraghni, N.F. Declercq, L. Guillaumat, G. Le Coz, S. Delalande, Detection and evaluation of barely visible impact damage in woven glass fabric reinforced polyamide 6.6/6 composites using ultrasonic imaging , X-ray tomography and optical profilometry, *Int. J. Damage Mech.* 30 (2020) 1–26. <https://doi.org/10.1177/1056789520957703>.
- [10] N. Hongkarnjanakul, Modélisation numérique pour la tolérance aux dommages d'impact sur stratifié composite : de l'impact à la résistance résiduelle en compression, (2013).
- [11] J. Holmes, S. Sommacal, Z. Stachurski, R. Das, P. Compston, Digital image and volume correlation with X-ray micro-computed tomography for deformation and damage characterisation of woven fibre-reinforced composites, *Compos. Struct.* 279 (2022) 114775. <https://doi.org/10.1016/J.COMPSTRUCT.2021.114775>.
- [12] A. Madra, N. El Hajj, M.L. Benzeggagh, X-ray microtomography applications for quantitative and qualitative analysis of porosity in woven glass fiber reinforced thermoplastic, *Compos. Sci. Technol.* 95 (2014) 50–58. <https://doi.org/10.1016/j.compscitech.2014.02.009>.
- [13] A. Maier, R. Schmidt, B. Oswald-Tranta, R. Schledjewski, Non-Destructive Thermography Analysis of Impact Damage on Large-Scale CFRP Automotive Parts, *Materials (Basel)*. 7 (2014) 413–429. <https://doi.org/10.3390/ma7010413>.
- [14] P. Pomarède, F. Meraghni, L. Peltier, S. Delalande, N.F. Declercq, Damage Evaluation in Woven Glass Reinforced Polyamide 6.6 / 6 Composites Using Ultrasound Phase-Shift Analysis and X-ray Tomography, *J. Nondestruct. Eval.* 37 (2018). <https://doi.org/10.1007/s10921-018-0467-3>.
- [15] Z. Su, L. Ye, Y. Lu, Guided Lamb waves for identification of damage in composite structures : A review, *J. Sound Vib.* 295 (2006) 753–780. <https://doi.org/10.1016/j.jsv.2006.01.020>.
- [16] S. Gholizadeh, A review of non-destructive testing methods of composite materials, in: *Procedia Struct. Integr.*, Elsevier B.V., 2016: pp. 50–57. <https://doi.org/10.1016/j.prostr.2016.02.008>.
- [17] C. Garnier, M.-L. Pastor, F. Eyma, B. Lorrain, The detection of aeronautical defects in situ on composite structures using Non Destructive Testing, *Compos. Struct.* 93 (2011) 1328–1336. <http://linkinghub.elsevier.com/retrieve/pii/S0263822310003594> (accessed November 30, 2014).
- [18] P.A. Howell, *Nondestructive Evaluation (NDE) Methods and Capabilities Handbook*, Langley Research Center, Hampton, Virginia February, 2020. <http://www.sti.nasa.gov> (accessed June 24, 2023).
- [19] J. Dong, A. Locquet, N.F. Declercq, D.S. Citrin, Polarization-resolved terahertz imaging of intra- and inter-laminar damages in hybrid fiber-reinforced composite laminate subject to low-velocity impact, *Compos. Part B Eng.* 92 (2016) 167–174. <https://doi.org/10.1016/j.compositesb.2016.02.016>.

- [20]G.J. Wilminck, J.E. Grundt, Current state of research on biological effects of terahertz radiation, *J. Infrared, Millimeter, Terahertz Waves* 32 (2011) 1074–1122. <https://doi.org/10.1007/S10762-011-9794-5/FIGURES/8>.
- [21]C. Jördens, M. Scheller, S. Wietzke, D. Romeike, C. Jansen, T. Zentgraf, K. Wiesauer, V. Reisecker, M. Koch, Terahertz spectroscopy to study the orientation of glass fibres in reinforced plastics, *Compos. Sci. Technol.* 70 (2010) 472–477. <https://doi.org/10.1016/j.compscitech.2009.11.022>.
- [22]J. Calvo-de la Rosa, P. Pomarède, P. Antonik, F. Meraghni, D.S. Citrin, D. Rontani, A. Locquet, Determination of the process-induced microstructure of woven glass fabric reinforced polyamide 6.6/6 composite using terahertz pulsed imaging, *NDT E Int.* (2023) 102799. <https://doi.org/10.1016/j.ndteint.2023.102799>.
- [23]M. Naftaly, R.E. Miles, Terahertz time-domain spectroscopy for material characterization, *Proc. IEEE* 95 (2007) 1658–1665. <https://doi.org/10.1109/JPROC.2007.898835>.
- [24]J. Dong, B. Kim, A. Locquet, P. McKeon, N.F. Declercq, D.S. Citrin, Nondestructive evaluation of forced delamination in glass fiber-reinforced composites by terahertz and ultrasonic waves, *Compos. Part B Eng.* 79 (2015) 667–675. <https://doi.org/10.1016/j.compositesb.2015.05.028>.
- [25]P. Lopato, T. Chady, Terahertz examination of fatigue loaded composite materials, *Int. J. Appl. Electromagn. Mech.* 45 (2014) 613–619. <https://doi.org/10.3233/JAE-141884>.
- [26]M. Radziński, M. Mieloszyk, E.K. Rahani, T. Kundu, W. Ostachowicz, Heat induced damage detection in composite materials by terahertz radiation, <https://doi.org/10.1117/12.2084144> 9438 (2015) 402–411. <https://doi.org/10.1117/12.2084144>.
- [27]F. Destic, C. Bouvet, Impact damages detection on composite materials by THz imaging, *Case Stud. Nondestruct. Test. Eval.* 6 (2016) 53–62. <https://www.sciencedirect.com/science/article/pii/S2214657116300351>.
- [28]P.H. Malinowski, W.M. Ostachowicz, F. Touchard, M. Boustie, L. Chocinski-Arnault, P.P. Gonzalez, L. Berthe, D. Silva de Vasconcellos, L. Sorrentino, Study of plant fibre composites with damage induced by laser and mechanical impacts, *Compos. Part B Eng.* 152 (2018) 209–219. <https://doi.org/10.1016/J.COMPOSITESB.2018.07.004>.